Ru(arene)(amino alcohol)-Catalyzed Transfer Hydrogenation of Ketones: Mechanism and Origin of Enantioselectivity

Diego A. Alonso,[†] Peter Brandt,[‡] Sofia J. M. Nordin,[†] and Pher G. Andersson*[,†]

Contribution from the Department of Organic Chemistry, Uppsala University, Box 531, S-751 21 Uppsala, Sweden, and Department of Medicinal Chemistry, Royal Danish School of Pharmacy, Universitetsparken 2, DK-2100 Copenhagen, Denmark

Received March 1, 1999

Abstract: The mechanism of the Ru(arene)(amino alcohol)-catalyzed transfer hydrogenation of ketones using isopropyl alcohol as the hydrogen source has been studied by means of hybrid density functional methods (B3PW91). Three mechanistic alternatives were evaluated, and it was shown that the reaction takes place via a six-membered transition state, where a metal-bound hydride and a proton of a coordinated amine are transferred simultaneously to the ketone. Further calculations provided a general rationale for the rate of the reaction by comparison of steric effects in the ground and transition states of the ruthenium hydride complex. It was found that the TS has a strong preference for planarity, and this in turn is dependent on the conformational behavior of the O,N-linkage of the amino alcohol ligand. Finally, a general model, rationalizing the enantioselectivity of the reaction, was developed. Experimental studies of both rate and enantioselectivity were used in order to support the computational results.

Introduction

Catalytic asymmetric hydrogenation of carbonyl groups to form chiral alcohols is one of the most frequently used methods in organic synthesis to create a new stereocenter. Recent developments in this field have been very successful, and a large number of catalytic methods have been developed to achieve this purpose.[1] Among these, the hydrogen transfer from isopropyl alcohol to ketones[2−5] is particularly useful due to its simplicity and the many favorable properties of the reductant.[5a] We have earlier developed a class of bicyclic 2-azanorbornyl-3-methanol ligands, which are readily available in both enantiomeric forms and combine high enantioselectivity with a fast rate of the hydrogen transfer reaction.[6]

In this work, we have performed a combined kinetics and quantum-chemical investigation in order to reveal the reaction mechanism and to understand the selectivity process of the reaction. The study is divided in three major parts: reaction mechanism, rate, and selectivity, denoted as sections I−III in the text. The aim of this study is to enable a rational design of ligands giving even higher selectivities and to further increase the rate of the reaction.

Computational Methods

All calculations reported in this work were conducted using the Gaussian 98 program.[7] Geometry optimizations were performed using B3PW91, a density functional type of calculation based on hybrid functionals,[8] together with the LANL2DZ ECP and basis set[9] (BSI). Intermediate energies were determined using B3PW91 together with the larger SDD[10] ECP and basis set included in Gaussian 98 (BSII). It should be noted that SDD, as it is defined in Gaussian 98, uses d95 for first row atoms. The final energies were determined using B3PW91 together with

[†] Uppsala University.

[‡] Royal Danish School of Pharmacy.

(1) (a) Noyori, R. *Asymmetric Catalysis in Organic Synthesis*; Wiley: New York, 1994; Chapter 2. (b) *Houben-Weyl, Methods of Organic Chemistry, Stereoselective Synthesis*; 4th ed., Helmchen, G. J., Schaumann, E., Eds.; Georg Thieme Verlag: Stuttgart, New York, 1995; Vol. E21d, pp 3945−4464.

(2) General references to transfer hydrogenation of ketones using *i*-PrOH: (a) Sasson, Y.; Blum, J. *Tetrahedron Lett.* **1971**, *24*, 2167. (b) Sasson, Y.; Blum, J. *J. Org. Chem.* **1975**, *40*, 1887. (c) Linn, D. E.; Halpern, G. *J. Am. Chem. Soc.* **1987**, *109*, 2969. (d) Chowdhury, R. L.; Bäckvall, J. E. *J. Chem. Soc., Chem. Commun.* **1991**, 1063.

(3) Asymmetric transfer hydrogenations: (a) Gladiali, S.; Pinna, L.; Delogu, G.; De Martin, S.; Zassinovich, G.; Mestroni, G. *Tetrahedron: Asymmetry* **1990**, *1*, 635. (b) Muller, D.; Umbricht, G.; Weber, B.; Pfaltz, A. *Helv. Chim. Acta* **1991**, *74*, 232. (c) Evans, D. A.; Nelson, S. G.; Gagné, M. R.; Muci, A. R. *J. Am. Chem. Soc.* **1993**, *115*, 9800. (d) Genet, J.-P.; Ratovelomonana-Vidal, V.; Pinel, C. *Synlett* **1993**, *34*, 478. (e) Krasik, P.; Alper, H. *Tetrahedron* **1994**, *50*, 4347. (f) Yang, H.; Alvarez, M.; Lugan, N.; Mathieu, R. *J. Chem. Soc., Chem. Commun.* **1995**, 1721. (g) Hashiguchi, S.; Fujii, A.; Takehara, J.; Ikariya, T.; Noyori, R. *J. Am. Chem. Soc.* **1995**, *117*, 7562. (h) Gamez, P.; Fache, F.; Lemaire, M. *Tetrahedron: Asymmetry* **1995**, *6*, 705. (i) Langer, T.; Helmchen, G. *Tetrahedron Lett.* **1996**, *37*, 1381. (j) Langer, T.; Janssen, J.; Helmchen, G. *Tetrahedron: Asymmetry* **1996**, *7*, 1599. (k) Jiang, Q.; Van Plew, D.; Murtuza, S.; Zhang, X. *Tetrahedron Lett.* **1996**, *37*, 797. (l) Püntener, K.; Schwink, L.; Knochel, P. *Tetrahedron Lett.* **1996**, *37*, 8165. (m) Gamez, P.; Dunjic, B.; Lemaire, M. *J. Org. Chem.* **1996**, *61*, 5196. (n) Gao, J.-X.; Ikariya, T.; Noyori, R. *Organometallics* **1996**, *15*, 1087. (o) Jiang, Y.; Jiang, Q.; Zhu, G.; Zhang, X. *Tetrahedron Lett.* **1997**, *38*, 215. (p) Sammakia, T.; Stangeland, E. L. *J. Org. Chem.* **1997**, *62*, 6104. (q) Matsumura, K.; Hashiguchi, S.; Ikariya, T.; Noyori, R. *J. Am. Chem. Soc.* **1997**, *119*, 8738. (r) Palmer, M.; Walsgrove, T.; Wills, M. *J. Org. Chem.* **1997**, *62*, 5226. (s) Inoue, S.-I.; Nomura, K.; Hashiguchi, S.; Noyori, R.; Izawa, Y. *Chem. Lett.* **1997**, 657. (t) Halle, R.; Schulz, E.; Lemaire, M. *Synlett* **1997**, 1257. (u) Touchard, F.; Fache, F.; Lemaire, M. *Tetrahedron: Asymmetry* **1997**, *8*, 3319. (v) Ohta, T.; Nakahara, S.; Shigemura, Y.; Hattori, K.; Furukawa, I. *Chem. Lett.* **1998**, 491. (w) Schwink, L.; Ireland, T.; Püntener, K.; Knochel, P. *Tetrahedron: Asymmetry* **1998**, *9*, 1143. (x) Bayston, D. J.; Travers, C. B.; Polywka, M. E. C. *Tetrahedron: Asymmetry* **1998**, *9*, 2015. (y) Jiang, Y.; Jiang, Q.; Zhang, X. *J. Am. Chem. Soc.* **1998**, *120*, 3817. (z) Everaere, K.; Carpentier, J.-F.; Mortreux, A.; Bulliard, M. *Tetrahedron: Asymmetry* **1998**, *9*, 2971. (aa) Breysse, E.; Pinel, C.; Lemaire, M. *Tetrahedron: Asymmetry* **1998**, *9*, 897. (bb) Arikawa, Y.; Ueoka, M.; Matoba, K.; Nishibayashi, Y.; Haidai, M.; Uemura, S. *J. Organomet. Chem.* **1999**, *572*, 163.

(4) Takehara, J.; Hashiguchi, S.; Fujii, A.; Inoue, S.; Ikariya, T.; Noyori, R. *Chem. Commun.* **1996**, 233.

(5) (a) Noyori, R.; Hashiguchi, S. *Acc. Chem. Res.* **1997**, *30*, 97. (b) Haack, K.-J.; Hashiguchi, S.; Fujii, A.; Ikariya, T.; Noyori, R. *Angew. Chem., Int. Ed. Engl.* **1997**, *36*, 285.

(6) Alonso, D. A.; Guijarro, D.; Pinho, P.; Temme, O.; Andersson, P. G. *J. Org. Chem.* **1998**, *63*, 2749.

10.1021/ja9906610 CCC: $18.00
Published on Web 10/04/1999

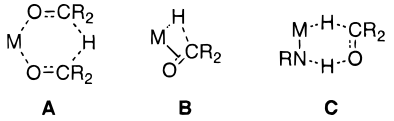

Figure 1. Three different mechanistic alternatives for metal-catalyzed transfer hydrogenation.

the 6-311+G** basis set for all atoms except for ruthenium, where SDD augmented with one f-polarization function was used (BSIII). An optimized f-polarization function was obtained by minimizing the B3PW91 energy of the free atom in the s^1d^7 ground state, resulting in an exponent of 1.1.[11] Hessians and zero-point corrections were calculated for some selected points using B3PW91/BSI. Solvation free energies were calculated in Gaussian 98 using the PCM method[12] with parameters for ethanol together with B3PW91 and SDD for ruthenium and 6-31G* for other atoms.

To facilitate the computational part of this study, the small 2-aminoethanol was used as ligand in the mechanistic study, whereas the 2-azanorbornyl-3-methanol ligands were used in the part where the kinetic aspects and the selectivity process were studied. The bicyclic ligands are well-suited for computational investigations due to their rigidity and their minimal conformational freedom.

Results and Discussion

I. Mechanism. Mechanistically, metal-catalyzed transfer hydrogenations may be divided into three main categories: (**A**) direct transfer of an α-hydrogen of an alcohol to the carbonyl carbon of a ketone, (**B**) migratory insertion (MI) of a coordinated ketone into a metal hydride bond, or (**C**) a concerted mechanism where a proton and a hydride are transferred simultaneously to the ketone, analogous to HN═NH reductions of unsaturated systems (Figure 1).[13] Transfer hydrogenation reactions involving a mild hydrogen donor such as isopropyl alcohol impose certain restrictions on the reaction thermodynamics. Since the reduction of acetophenone by *i*-PrOH is almost thermoneutral,[14] a very narrow energetic window is available for all involved intermediates not to inhibit the reaction. Thermodynamically well balanced reaction steps are thus crucial for the catalyst turnover rate, and all reactions should be close to thermoneutral.

A mechanism such as **A**, involving a direct transfer of a hydride from a metal-coordinated alkoxide to a coordinated ketone, is the generally accepted mechanism for aluminum(III)-catalyzed Meerwein−Ponndorf−Verley reduction of ketones.[14] It is also the presumed mechanism of the iridium(I)-catalyzed transfer hydrogenation of ketones.[15] A mechanism such as **B** has been invoked in the analogous rhodium(I) reaction[3a,16] and has also been suggested to be the mechanism for some ruthenium(II)-catalyzed transfer hydrogenations using ligands other than arenes.[17] Recently, Noyori et al. proposed a concerted mechanism of type **C** for the reduction of ketones by Ru(II) arene complexes with bidentate amino alcohol or amino sulfonamide ligands,[5] a conclusion based on experimental observations. To assign confidently a mechanism to the title reaction, we examined all three alternatives.

Scheme 1. Mechanistic Proposal Involving a Direct Transfer of a Hydride, **TS A**

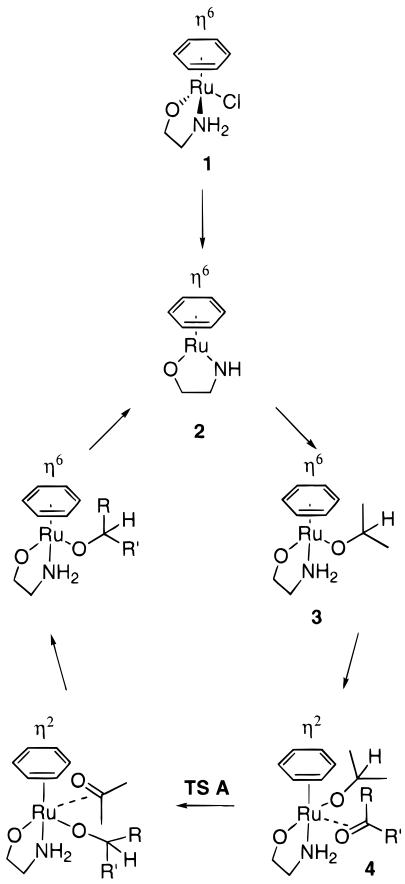

Direct Transfer of a Hydride: Mechanism A. A mechanistic proposal involving a direct transfer of a hydride (**TS A**) is depicted in Scheme 1, and the energies of the stationary points on the potential energy surface (PES) are given in Table 1. The geometry of **TS A** is shown in Figure 2.

The catalytic cycle hypothesized in Scheme 1 starts with the formation of a very stable isopropoxyruthenium complex, **3**. The transition state for the formation of this intermediate could not be located, and optimizations starting from a loosely coordinated isopropyl alcohol resulted in a barrierless proton

(7) Frisch, M. J.; Trucks, G. W.; Schlegel, H. B.; Scuseria, G. E.; Robb, M. A.; Cheeseman, J. R.; Zakrzewski, V. G.; Montgomery, J. A.; Stratmann, R. E., Jr.; Burant, J. C.; Dapprich, S.; Millam, J. M.; Daniels, A. D.; Kudin, K. N.; Strain, M. C.; Farkas, O.; Tomasi, J.; Barone, V.; Cossi, M.; Cammi, R.; Mennucci, B.; Pomelli, C.; Adamo, C.; Clifford, S.; Ochterski, J.; Petersson, G. A.; Ayala, P. Y.; Cui, Q.; Morokuma, K.; Malick, D. K.; Rabuck, A. D.; Raghavachari, K.; Foresman, J. B.; Cioslowski, J.; Ortiz, J. V.; Stefanov, B. B.; Liu, G.; Liashenko, A.; Piskorz, P.; Komaromi, I.; Gomperts, R.; Martin, R. L.; Fox, D. J.; Keith, T.; Al-Laham, M. A.; Peng, C. Y.; Nanayakkara, A.; Gonzalez, C.; Challacombe, M.; Gill, P. M. W.; Johnson, B.; Chen, W.; Wong, M. W.; Andres, J. L.; Gonzalez, C.; Head-Gordon, M.; Replogle, E. S.; Pople, J. A. Gaussian 98, Revision A.3; Gaussian, Inc., Pittsburgh, PA, 1998.

(8) Becke, A. D. *J. Chem. Phys.* **1993**, *98*, 5648. Perdew, J. P.; Wang, Y. *Phys. Rev. B*, **1992**, *45*, 13244.

(9) Hay, P. J.; Wadt, W. R. *J. Chem. Phys.* **1985**, *82*, 299.

(10) Andrae, D.; Häussermann, U.; Dolg, M.; Stoll, H.; Preuss, H. *Theor. Chim. Acta* **1990**, *77*, 123.

(11) For a similar determination, see: Ehlers, E. W.; Böhme, M.; Dapprich, S.; Gobbi, A.; Höllwarth, A.; Jonas, V.; Köhler, K. F.; Stegmann, R.; Veldkamp, A.; Frenking, G. *Chem. Phys. Lett.* **1993**, *208*, 111.

(12) Tomasi, J.; Persico, M. *Chem. Rev.* **1994**, *94*, 2027−2094.

(13) For an excellent review, see: Gladiali, S.; Mestroni, G. In *Transition Metals for Organic Synthesis*: Beller, M., Bolm, C., Eds.; Wiley-VCH: Weinheim, Germany, 1998; Vol. 2, pp 97−119.

(14) de Graauw, C. F.; Peters, J. A.; van Bekkum, H.; Huskens, J. *Synthesis* **1994**, 1007.

(15) Zassunovich, G.; Bettella, R.; Mestroni, G.; Bresciani-Pahor, N.; Geremia, S.; Randaccio, L. *J. Organomet. Chem.* **1989**, *370*, 187.

(16) Bernard, M.; Guiral, V.; Delbecq, F.; Fache, Sautet, P.; Lemaire, M. *J. Am. Chem. Soc.* **1998**, *120*, 1441.

(17) Bäckvall, J.-E.; Chowdhuri, R. L.; Karlsson, U.; Wang, G. Z. In *Perspectives in Coordination Chemistry*; Williams, A. F., Floriani, C., Merbach, G., Eds.; Verlag Helvetica Chimica Acta: Basel, Switzerland, 1992; p 463.

Table 1. Potential Energy Surface of the Reaction Shown in Scheme 1 (kcal/mol)

species	relative energy[a] BS I	BS II	BS III
2	6.3	3.7	3.3
2-*i*-PrOH[b]	0.0	0.0	0.0
3	−10.3	−7.8	−5.8
4[c]			
TS A	11.7	15.0	30.8

[a] The basis sets are described in Computational Details. ZPE corrections were calculated at B3PW91/BS I. [b] A hydrogen-bonded molecular complex. [c] This specieswas found to be a nonstationary point on the PES.

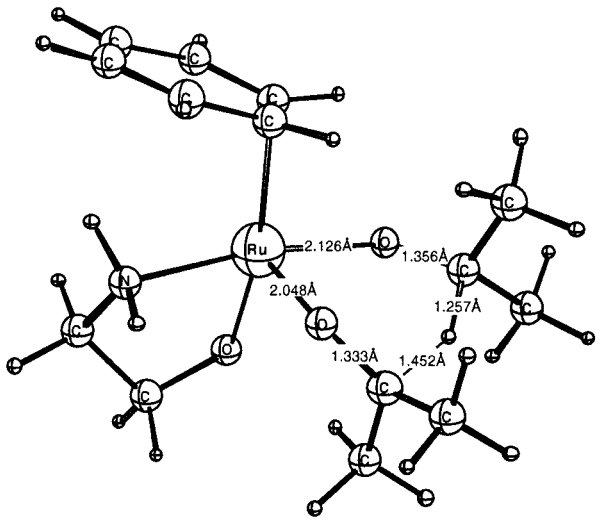

Figure 2. The lowest transition state for a direct transfer of a hydride from the hydrogen donor alcohol **TS A** (B3PW91/BS I).

transfer to the amide nitrogen. The next step in the reaction, according to the proposal in Scheme 1, is coordination of a ketone to the ruthenium. In our attempts to find π-complexes of this type, **4**, all structures were optimized to geometries where the benzene ligand is released. We could nevertheless locate a TS for the proposed hydride transfer as a high-energy point on the PES. Whether this TS couples to a π- or σ-acetone complex or to a complex where the acetone is expelled was not evaluated. Earlier studies have shown that the stereochemical outcome of the reaction is independent of the chirality of the hydrogen donor.[5b] This strongly suggests that a mechanism involving a direct transfer of a hydride is not operative in this reaction. In addition to the very high energy found for **TS A**, this mechanistic alternative can confidently be ruled out. The increase in energy of **TS A** is in part due to a better description of the ground-state η^6-coordinated benzene, using a polarized basis set such BSIII.

Migratory Insertion of a π-Bound Ketone into a Metal Hydride: Mechanism B. A mechanistic proposal based on a migratory insertion step is shown in Scheme 2 , and the corresponding PES is given in Table 2.

Also in this case, the reaction starts by formation of the stable isopropoxy ruthenium complex **3**. The next step in the reaction is slippage of the arene ligand from η^6 to η^2, allowing the formation of an agostic interaction between the α-hydrogen of the alkoxide and ruthenium (**5**).[18] The TS for this process was not located in the study. Subsequent β-elimination via **TS B** (Figure 3) leads to ruthenium hydride **6** with a π-bound ketone. Energetically, both the β-agostic intermediate **4** and the TS for the MI/β-elimination (**TS B**) were found to be rather high in energy compared to the hydrogen-bonded molecular complex **2-*i*-PrOH**.[19] As seen in Table 2, the change in coordination from η^6-benzene to η^2-benzene is unfavorable and also shows a rather large basis set dependence. Apparently, polarization functions are needed in order to describe the *energy* of this change in hapticity.

Concerted Transfer of both a Proton and a Hydride: Mechanism C. This mechanism has recently been proposed by Noyori and involves only two different ruthenium complexes connected by a single transition state (Scheme 3).[5] The TS was difficult to locate for the smallest systems used in this study, and the PES around **TS C** was found to be flat. A frequency calculation showed one imaginary frequency as expected for a TS (Figure 4). An IRC calculation supports the conclusion about the flat shape of the PES and the characterization of the stationary point as a TS. The energies are shown in Table 3. The activation energy found for this reaction pathway was only 12.9 kcal/mol, and the conclusion is that the reaction takes place in this manner and not via a migratory insertion or a direct hydride transfer.

Mechanistic Conclusions. The hydride transfer step in the three different mechanisms described above differs significantly in energy. The activation energies of **TS A**−**C** were found to be 30.8, 20.1, and 12.9 kcal/mol, respectively. On the basis of these energies, mechanisms **A** and **B** could both be ruled out. Some transition states and intermediates remain to be identified for these two mechanisms, but irrespective of the energies of those, the actual hydride transfer step will always inhibit these pathways. Thereby, the mechanism **C**, initially proposed by Noyori, can confidently be assigned to the Ru(arene)(amino alcohol)-catalyzed transfer hydrogenation of ketones.

II. Kinetics. A large range of different ligands has been evaluated in the Ru(arene)-catalyzed transfer hydrogenation.[13] Among these, the aminoethanol-based ligands resulted in the largest ligand acceleration,[4,5a] but the rates depend critically on the specific structure of the ligand. As for the bicyclic ligand **9**, the rate is highly dependent on the substitution pattern of the carbinol carbon.[6] To understand how steric factors influence the rate of the reaction, we decided to study this both by experiment and by means of quantum-chemical calculations.

The activation energies of hydrogen transfer were calculated using **TS C** and four different amino alcohol ligands (Figure 5) in combination with benzene or dimethylbenzene (DMB) as the arene ligands. In addition to the computational study, rates were measured by means of spectrophotometry for the reactions catalyzed by the bicyclic ligand **9** in combination with benzene, *p*-cymene, and hexamethylbenzene (HMB) as the arene ligands. The rate was also measured for the *p*-cymene-based catalysts of ligands **10** and **11**, where a methyl substituent has been introduced at the carbinol carbon. The results are shown in Table 4, and an illustration showing the decay of the acetophenone absorption is given in Figure 6.

Effects on the Rate due to Arene Substitution. Experimentally, we found transfer hydrogenations using ligand **8** and benzene troublesome to perform and the results were variable.[20]

(18) Complexes **4** and **5** could potentially form η^4-benzene complexes. All attempts to locate such species resulted, however, in the formation of less strained η^2-coordinated benzene complexes. In complexes **1**−**3** and **6**, the benzene ligand was found to be η^6-coordinated.

(19) In the study of both mechanisms **A** and **B**, a number of different configurations around ruthenium were evaluated in order to find the lowest energy pathway.

(20) The ruthenium complex of 2-aminoethanol and benzene has been shown to be very labile and tends to decompose during the reaction. This reaction has earlier been reported to have a TOF of 227 h^{-1}.[5a]

Scheme 2. Mechanistic Proposal Involving a Migratory Insertion of a π-Bound Ketone into a Metal Hydride

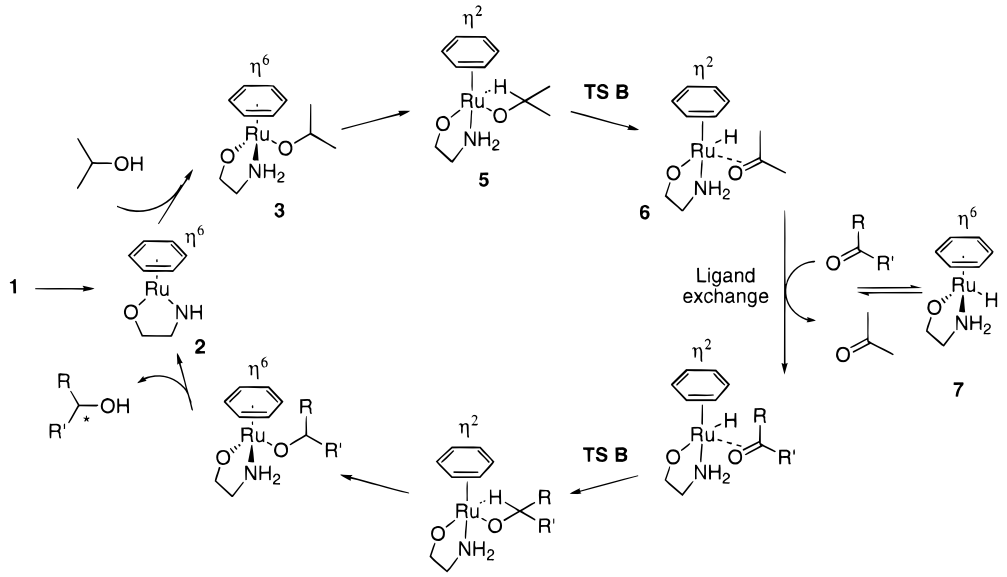

Table 2. Potential Energy Surface of the Reaction Shown in Scheme 2 (kcal/mol)

species	relative energy[a] BS I	BS II	BS III
2	7.3	8.3	6.1
2-*i*-PrOH[b]	1.0	4.6	2.8
3	−8.7	−6.9	−1.2
5	9.2	16.3	23.6
TS B	10.8	16.1	20.1
6	9.2	8.7	14.2
7-acetone[b]	0.0	0.0	0.0
7	7.4	10.3	6.3

[a] The basis sets are described in Computational Details. ZPE corrections were calculated at B3PW91/BS I. [b] Hydrogen-bonded molecular complexes.

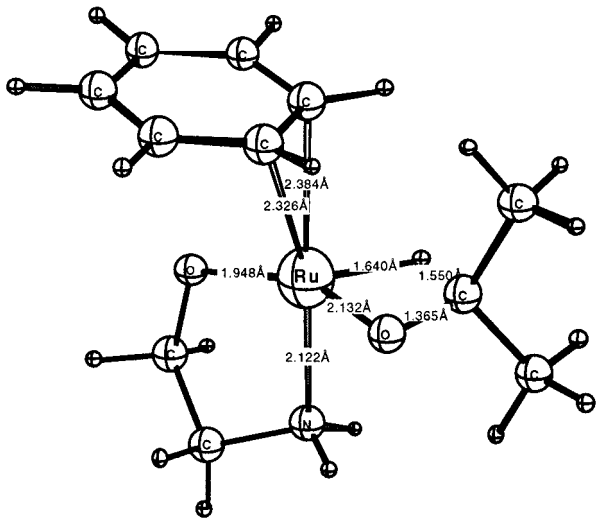

Figure 3. The lowest transition state found involving a migratory insertion, **TS B** (B3PW91/BS I).

This ligand combination was nevertheless used in the computational part of the study in order to enable an evaluation of the effects of arene substitution. As seen in Table 4, entries 1 and 2, the calculations indicate that arene substitution at positions facing the ketone should lead to an increase in the activation energy of hydrogen transfer. This effect is observed experimentally for ligand **9** when benzene is exchanged for a HMB ligand (Table 4, entries 3 and 5), whereas the 1,4-disubstituted *p*-cymene complex (entry 4) shows a rate similar to that for the benzene complex.

Scheme 3. Catalytic Cycle of the Mechanism Involving a Concerted Transfer of both a Proton and a Hydride (Mechanism **C**)

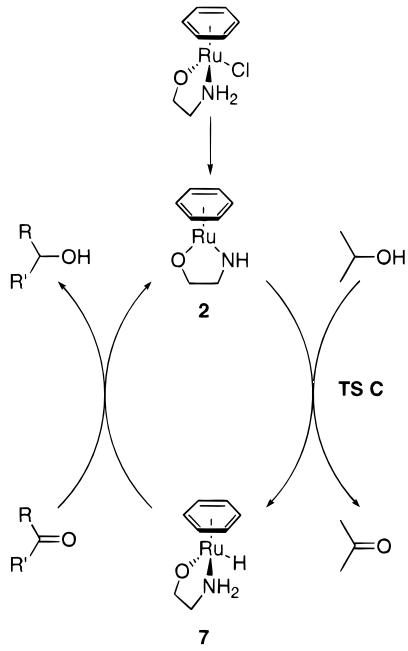

Effects on the Rate due to Substitutions at the Carbinol Carbon. A set of calculations was performed on different conformations of both the ruthenium hydride and the corresponding pro-(*S*)-TS. The results are illustrated graphically in Figure 7, 9, and 10 (vide infra). Starting with the ruthenium hydride complexes of ligands **8**−**11**, these were all found to exist in two different conformations, denoted α and β in the following text. Either the carbinol carbon is pointing toward the hydride (α) or it is pointing away from the hydride (β). All ruthenium hydride complexes showed a preference for the α-conformation possibly due to a more favorable binding to ruthenium (Figure 7). It was found that the relative energies between the α- and β-conformations are very sensitive to substitution at the carbinol carbon. When even such a small

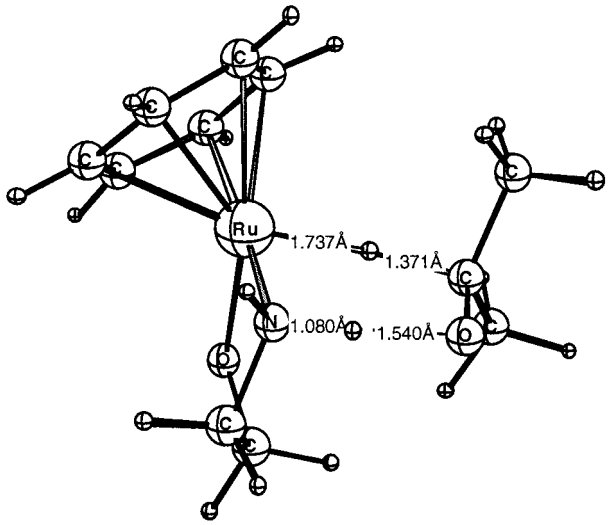

Figure 4. Concerted transfer of both a proton and a hydride, **TS C** (B3PW91/BS I).

Table 3. Potential Energy Surface of the Reaction Depicted in Scheme 3 (kcal/mol)

species	relative energy[a]		
	BS I	BS II	BS III
2	7.3	8.3	6.1
2-*i*-PrOH[b]	1.0	4.6	2.8
TS C	9.8	12.3	12.9
7-acetone[b]	0.0	0.0	0.0
7	7.4	10.3	6.3

[a] The basis sets are described in Computational Details. ZPE corrections were calculated at B3PW91/BS I. [b] Hydrogen-bonded molecular complexes.

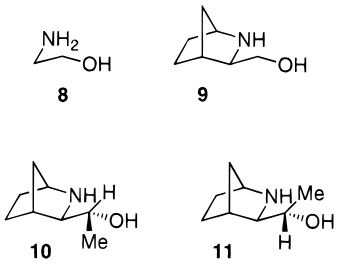

Figure 5. Ligands used in the kinetic study.

group as a methyl is introduced, the relative energies of the two conformers could be modulated in a range of 1.7−7.5 kcal/mol (Figures 7 and 10). This effect was found to be of importance for the rate of the reaction (vide infra) and could readily be explained in terms of steric interactions between either the (*R*)-methyl group of ligand **10** and the hydride in the α-conformation or between the (*S*)-methyl group of ligand **11** and the arene ligand in the *β*-conformation.

An analysis of the conformational preference in the TS of each catalyst, showed that the favored TS conformations did not correlate in a straightforward manner with the lowest energy conformer of the ruthenium hydride ground states (Figures 8−10). Instead, a new factor was found to be responsible for the energetic differentiation of the conformers, namely the H−Ru−N−H dihedral angle, which shows a strong preference for being planar. The planarity of the TS is controlled by the conformation of the ligand, which in turn affects the H−Ru−N−H dihedral angle (Figure 8). In fact, there is a very good linear correlation between this angle and the energy of the TS for ligands **8** and **9** (Figure 11). This dihedral effect determines

Table 4. Rate Constants for Hydrogen Transfer to Acetophenone and Calculated Activation Energies Relative to the Corresponding Ruthenium Hydride Complex 7 (Δ*E*, B3PW91/BS III//B3PW91/BS I)

entry	ligand[a]	$1000k^b$ (min^{-1})	$\Delta E^{\ddagger c}$ (kcal/mol)		
			BS I	BS II	BS III
1	**8**+**benzene**		4.0	3.6	7.7
2	**8**+**DMB**		5.2	5.0	10.6
3	**9**+**benzene**	ca. 29	4.6	4.6	8.0
4	**9**+***p*-cymene**	30			
5	**9**+**HMB**	9			
6	**10**+***p*-cymene**[d]	70	3.1	2.8	5.7
7	**11**+***p*-cymene**[d]	17	8.0	7.6	11.5

[a] In entries 6 and 7 benzene was used in the calculations. [b] The pseudo-first-order rate constants are given assuming a steady-state concentration of the ruthenium hydride complex. The catalyst in entry 7 shows an initial zero-order rate dependence, and the first-order fit was done in the final interval starting from 150 min. [c] The energies refer to the formation of the major isomer of 1-phenylethanol, i.e., the *S* isomer. [d] The enantiomeric excess achieved in the reaction in entry 6 using ligand **10** was 93.5%, and the ee in the reaction catalyzed by ligand **11** in entry 7 was 85%.

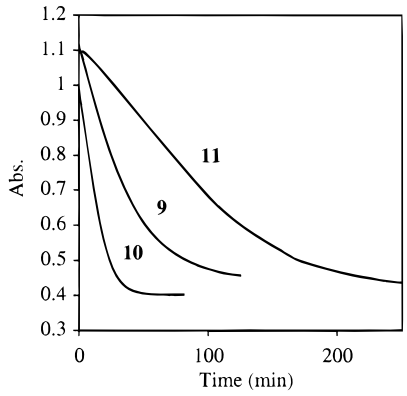

Figure 6. Kinetic traces for the reduction of acetophenone using Ru(*p*-cymene)(**9**−**11**)Cl as catalyst precursor.

the conformation of the ligand in the transition states of the reactions involving ligands **8**−**10** but has no effect on the conformation of the respective ruthenium hydride complexes. In the TS involving ligand **11**, a severe steric interaction between the (*S*)-methyl substituent and the arene is raising the energy of the *β*-conformation in the TS to an energy very close to the energy of the α-conformation (Figures 9 and 10). Thus, the rate drops for the reaction promoted by ligand **11** compared to those promoted by ligands **8**−**10** having *β*-conformations of low energy in the TSs. The higher rate of the reaction with ligand **10** compared to ligand **9** is due to a destabilization of the generally favored α-conformation of the ruthenium hydride ground state having the carbinol carbon pointing toward the hydride (Figure 7). The surprising effect found experimentally, that the introduction of an (*R*)-methyl substituent facing the aryl ketone increased the reaction rate, could thus be fully explained by the calculations using **TS C**.

The conformational analysis of ligand **8** in **TS C** (Figure 8) could serve as a basis for the kinetic analysis of acyclic 1,2-disubstituted 2-amino alcohols such as ephedrine. In such catalysts, the α-conformation of the TS could be expected to be lowest in energy and the carbinol substituent should be placed in an equatorial position. Using this rationale, it is possible to correctly predict and understand the selectivity in the formation of the ruthenium hydride.

III. Selectivity. The selectivity of the transfer hydrogenation has not yet been satisfactorily rationalized, although a consider-

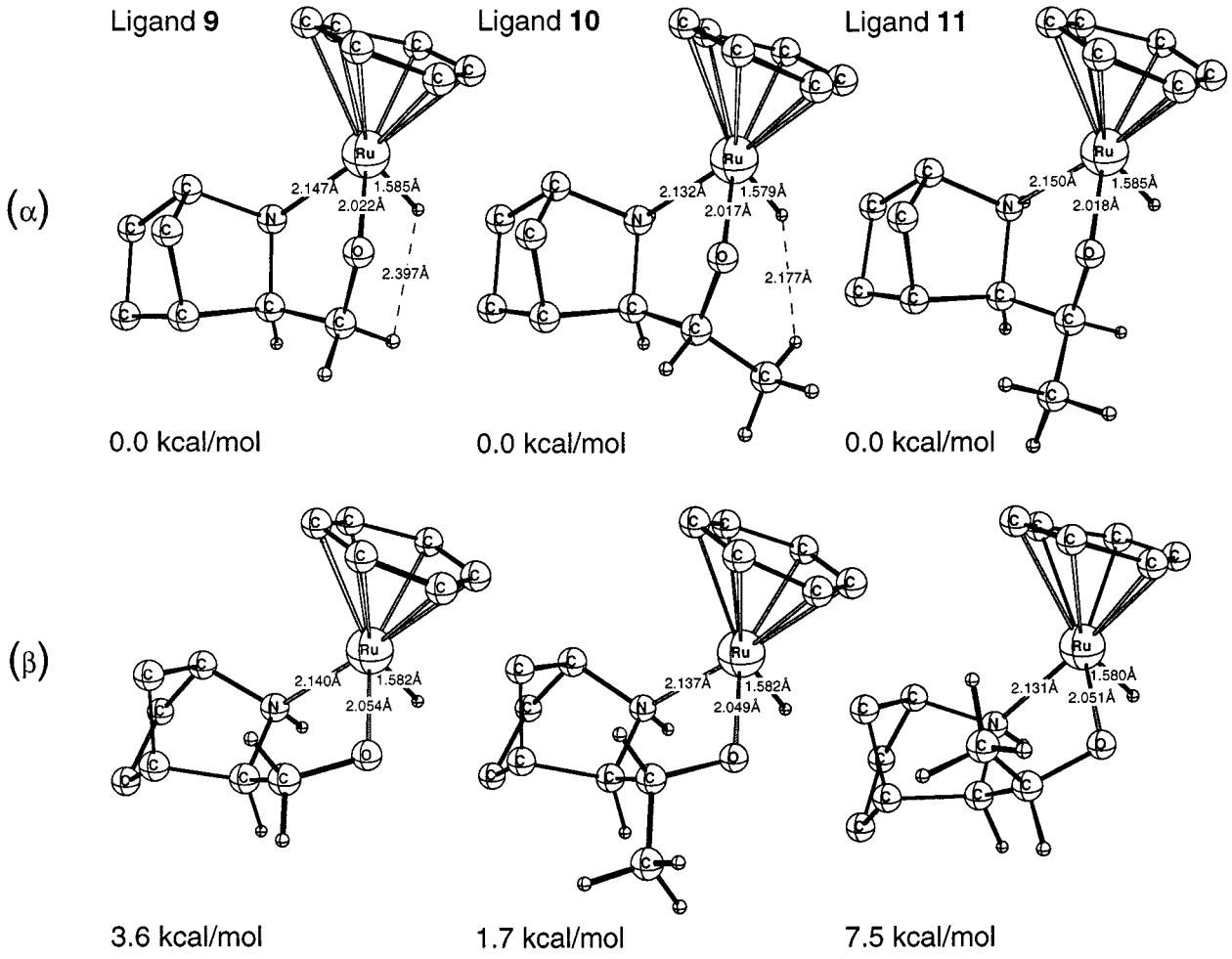

Figure 7. Relative energies of conformeric ruthenium hydride complexes of ligands **9**−**11** (B3PW91/BS I). α and *β* refer to the different conformations of the ligand (vide supra). The (*R*)-methyl group of ligand **10** causes selective destabilization of the α-conformation, whereas the (*S*)-methyl group of ligand **11** destabilizes the *β*-conformation.

able amount of ligands and catalytic systems have been studied.[13] It has recently been suggested by Noyori that carbonyl lone pair discrimination affected by a hydrogen bond to the amine N−H group of the ligand could provide an explanation to the enantioselection in the TS.[5a] This is, however, in conflict with a concerted transfer of both a proton and a hydride to the ketone since, in that case, the lone pair of the carbonyl oxygen is not involved in any hydrogen bond interaction in the TS. Instead, the proton and the hydride are transferred to the *π*-face of the ketone. To find the reasons behind the enantioselectivity, the selectivity was evaluated using two different amino alcohol ligands on ruthenium: first, 2-aminoethanol **8** and then the bicyclic 2-azanorbornyl-3-methanol **9** (Figure 5), which was also evaluated experimentally.

In the case of the ligand **9**, it has been shown in other reactions that the face selectivity at the amide nitrogen is complete when the ligand is coordinated to a metal.[21] For the ruthenium-catalyzed transfer hydrogenation, the energy between the two diastereomeric forms of the Ru(benzene)-**9** hydride species was determined to be 12 kcal/mol (Figure 12, B3PW91/BS I). The evaluation of the enantioselectivity was performed using the same configuration at the ruthenium center for both ligands **8** and **9**: i.e., the configuration depicted in Figure 8. The results are presented in Table 5.

Gas-Phase Selectivity (BS III). Assuming 2-aminoethanol to be a reasonably good model for ephedrine analogues, the results presented in Table 5 clearly show that a gas-phase treatment of the reaction is not sufficient for a correct prediction of the enantioselectivity of the reaction. The role of substituents on the arene ligand has been extensively studied experimentally,[4] and the results from that investigation demonstrate that the use of a benzene ligand is disadvantageous and an increased size of the arene is beneficial for the selectivity. It may thus be concluded that the enantioselectivity of the reaction is governed by factors *not* included in the gas-phase calculations and that solvent effects are necessary for a correct description of this process.

Solvent Effects on the Selectivity. One way of taking the reaction media into account is to perform single-point calculations using an appropriate solvent model. Although absolute solvation energies usually are difficult to predict with high accuracy, the difference in solvation between diastereomeric transition states could be expected to be better described. In this paper we chose the polarized continuum model (PCM) included in the Gaussian 98 program package to estimate the solvation free energies.[12] As seen in Table 5, the PCM calculations indicate that a chiral center at ruthenium indeed should be sufficient to turn the reaction highly enantioselective.

(21) (a) Brandt, P.; Hedberg, C.; Lawonn, K.; Pinho, P.; Andersson. P. G. *Chem. Eur. J.* **1999**, *5*, 1692. (b) Brandt, P.; Andersson, P. G. Unpublished results on the mechanism of the rearrangement of epoxides into allylic alcohols. See: Södergren, M.; Andersson, P. A. *J. Am. Chem. Soc.* **1998**, *120*, 10760.

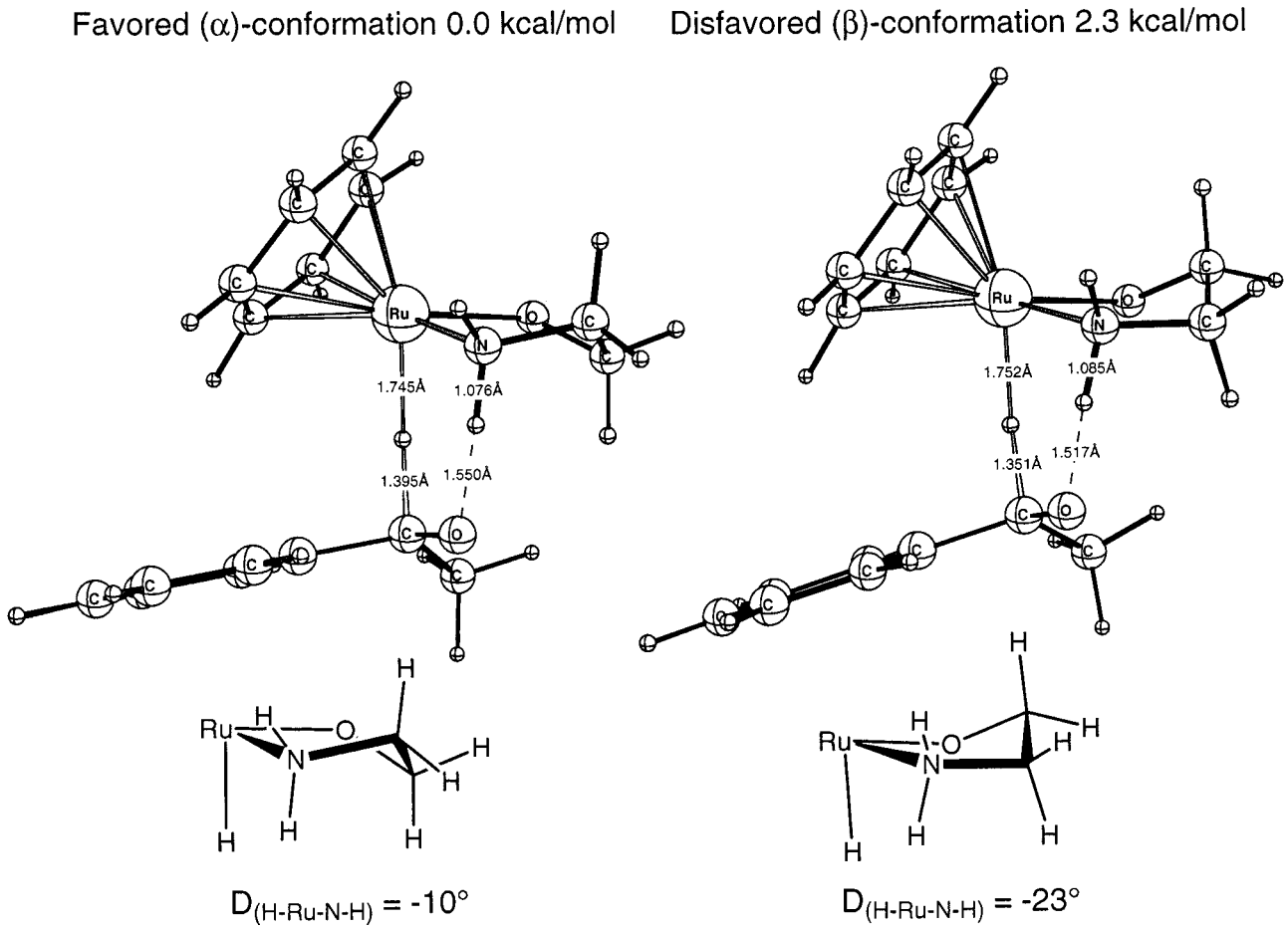

Figure 8. Two different conformers of **TS C** (ligand **8**) possessing differences in the planarity of the H−Ru−N−H reaction core. Relative energies were calculated at B3PW91/BS I.

This is an important piece of information that in combination with the conformational analysis of the ethylene bridge described in the kinetic part of this work nicely explains the selectivity of acyclic 2-amino alcohols such as ephedrine and analogues thereof. Most interestingly, the effect of exchanging the benzene for an HMB (modeled by DMB) is correctly described (Table 5, entry 2). The solvent effect on the larger model system using ligand **9** is smaller but points in the same direction as the PCM calculations performed for ligand **8**.

Conclusions

In this paper, we have investigated the mechanism of the Ru(arene)(*β*-amino alcohol)-catalyzed transfer hydrogenation of aromatic ketones, both by experiment and by means of quantum-chemical calculations. We have been able to rule out two mechanistic alternatives: one involving a direct hydride transfer from the alcohol hydrogen donor to the ketone and the other involving a migratory insertion of a ketone into a ruthenium−hydride bond. A third mechanistic alternative first suggested by Noyori, involving a concerted transfer of both a hydride and a proton from the catalyst to the ketone, was found to be the mechanism of this reaction.

We have further investigated how the rate of the reaction is affected by the ligand architecture and found a very strong preference for a planar H−Ru−N−H moiety. We have also been able to identify structural features of the ruthenium hydride, which is important for the overall rate. The rates measured experimentally for our 2-azanorbornyl-3-methanol ligands (**9**−**11**) were found to correlate with activation energies calculated by quantum-chemical methods. In the final part of this study we were able to rationalize the product selectivity in terms of two different steps. First, generation of an enantiopure ruthenium center is accomplished by the chiral ligand. This may be achieved by the use of a rigid ligand that strongly disfavors one specific configuration of the coordinated NH group or introduces a substituent at the carbinol carbon of the amino-ethanol backbone. The second step in the enantioselection is a differentiation of the two enantiofaces of the acetophenone by means of a ligand-specific combination of steric and solvent effects. In particular, the correlation between increased size of the arene ligand (hexamethylbenzene instead of benzene) is nicely explained by solvation. On the basis of the comprehensive knowledge presented in this paper, we are currently exploring some of the ideas of this new rate/selectivity model in our search for better catalysts. Finally, we would like to emphasize that the conclusions derived in this study should in principle be applicable to all Ru(arene)-catalyzed transfer hydrogenations using amino alcohols.

Experimental Section

For general experimental information see ref 22. HPLC analyses on (*S*)-α-methylbenzyl alcohol were carried out on a chiral column (ChiralCel OD-H) using a 254 nm UV detector and a flow rate of 0.5 mL/min of 5% *i*-PrOH in hexane. Kinetic measurements were performed on a Varian Cary 3 BIO UV−vis spectrophotometer equipped with a temperature controller thermostat. The temperature

(22) Bedekar, A. V.; Koroleva, E. B.; Andersson, P. G. *J. Org. Chem.* **1997**, *62*, 2518.

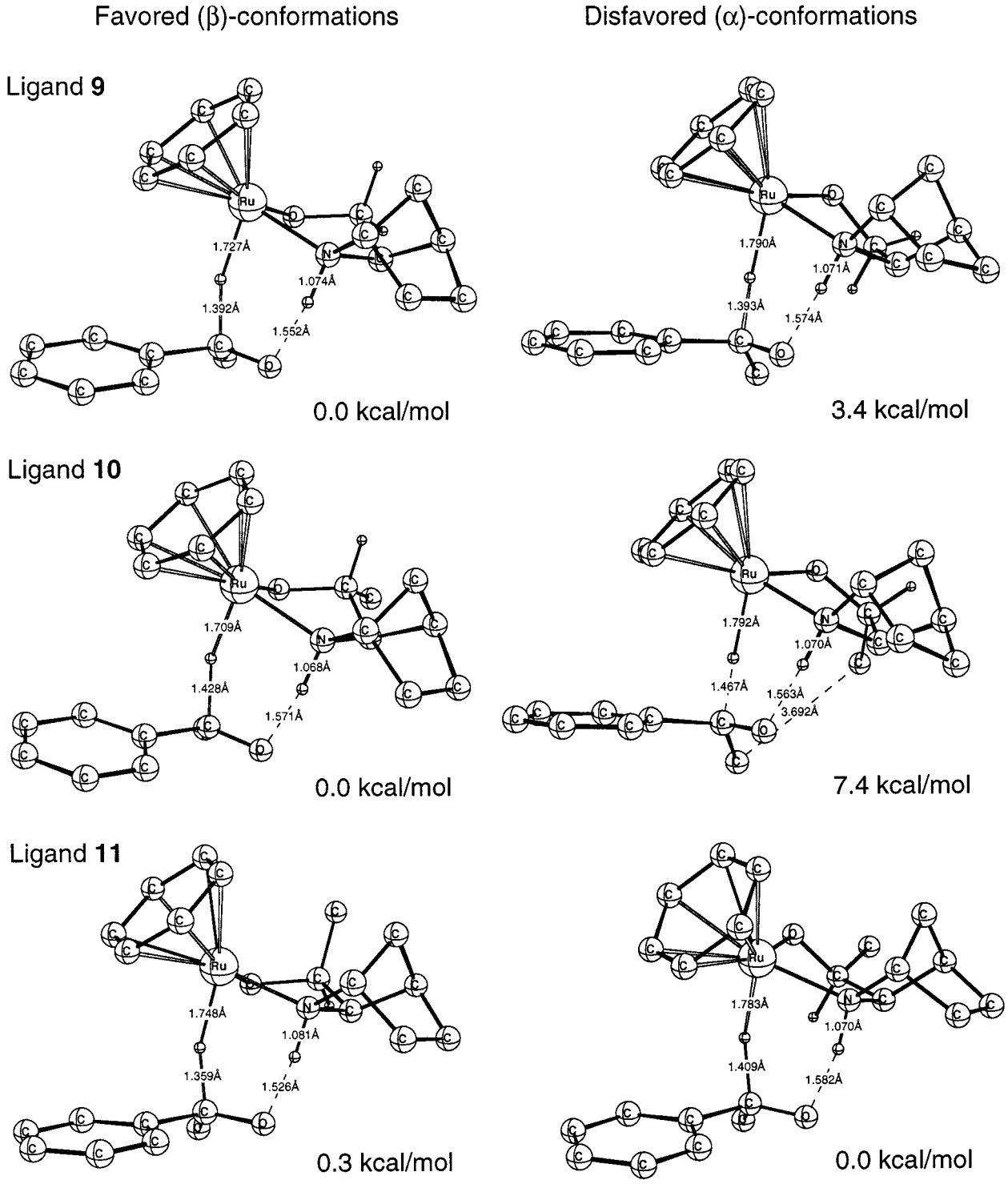

Figure 9. Relative activation energies of conformeric TS using ligands **9**−**11** (B3PW91/BS I). α and *β* refer to the different conformations of the ligand (vide supra). The (*S*)-methyl group of ligand **11** causes selective destabilization of the *β*-conformation of the TS, thereby lowering the rate of the reaction (B3PW91/BS I).

was measured with a digital thermometer (±0.1 °C) with type K thermal couple wire. The reactions were monitored at 310 nm at 25 °C, and first-order rate constants were calculated using the procedure included in the Cary WinUV program (absorbance of acetophenone versus time).

Synthesis of Ligands. Ligands **9**,[6] **10**,[21] and **11**[21] were prepared according to the literature procedures.

(1*S*,3*R*,4*R*)-2-Azabicyclo[2.2.1]heptane-3-(*R*)-methylmethanol (9): mp (hexane/ether) 159−160 °C; $[\alpha]^{25}_{D} = -50$ ($c = 0.2$, $CHCl_3$); IR (KBr) 3387, 2970, 1541, 1411 cm^{-1}; ^1H NMR δ 1.14 (3H, d, $J =$ 6.4 Hz), 1.20 (1H, d, $J = 10$ Hz), 1.36−1.44 (2H, m), 1.58−1.71 (4H, m), 2.21 (1H, br s), 2.49 (1H, d, $J = 8.4$ Hz), 3.26 (1H, m), 3.54 (1H, br s), 3.89 (1H, m); ^{13}C NMR δ 20.4, 28.4, 32.1, 34.7, 38.9, 56.0, 67.9, 68.3; MS (70 eV, EI; *m*/*z*): 141 (M^+, 35%), 140 ($M^+ - 1$, 55), 111 (80), 110 (100), 96 (23), 94 (23), 83 (28), 82 (55), 81 (32), 80 (27), 69 (34), 68 (52), and 67 (22).

Transfer Hydrogenation of Acetophenone. General Procedure. The ruthenium complex dimer (0.25 mol %) and the corresponding ligand (2 mol %) were weighed into a round-bottom flask, and any moisture was azeotropically removed via evaporation of benzene (5 × 5 mL) at reduced pressure. A condenser was attached, and the residue was dissolved in dry (freshly distilled from $CaCl_2$) *i*-PrOH (3 mL). The solution was refluxed under nitrogen for 30 min before it was

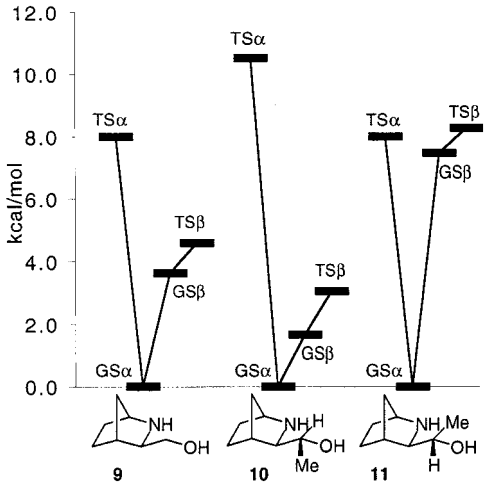

Figure 10. Activation energies (TS) and energies of the ruthenium hydride ground states (GS) for different conformeric pathways (B3PW91/BS I). α and *β* refer to the different conformations of the ligand (vide supra).

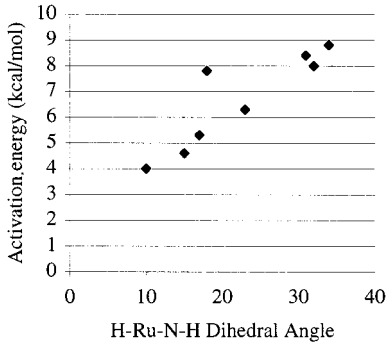

Figure 11. Correlation between the activation energy of the hydrogen transfer and the H−Ru−N−H dihedral angle for ligands **8** and **9**, two diastereomeric TS with two different conformations.

Table 5. Evaluation of the Selectivity in the Reduction of Acetophenone Starting from an Enantiomerically Pure Ruthenium Hydride (*7*)

entry	**TS C** derived from ligand	% ee (*S*)	energy (*R*−*S*)[a] (kcal/mol) BS I	BS II	BS III	PCM[d]
1	**8**+**benzene**		1.3	1.1	0.5	4.0
2	**8**+**DMB**[b]		1.5	1.6	−0.5	5.6
3	**9**+**benzene**	77	3.2	3.0	2.2	3.2
4	**9**+***p*-cymene**	94				
5	**9**+**HMB**[c]	95				

[a] Geometries at B3PW91/BS I. [b] DMB = 1,2-dimethylbenzene. This ligand was rotated in such a way that the methyl groups were facing the phenyl of the acetophenone. [c] HMB = hexamethylbenzene. [d] The free energy of solvation as calculated by PCM was added to the energy at BS III.

cooled to room temperature and transferred to a flask containing a solution of the ketone (1 mmol) and potassium isopropoxide (2.5 mol %) in *i*-PrOH (7 mL). The resulting solution was then stirred for 1.5 h at room temperature under nitrogen (monitored by GC and/or ^{1}H NMR), neutralized with a 1 M solution of HCl, and concentrated in vacuo to give the crude product, which after dilution on EtOAc and filtration over a thin pad of Celite was analytically analyzed.

Kinetic Measurements. For all kinetic experiments, the following procedure was applied: immediately after the addition of the catalyst over the acetophenone−base solution (see above) a sample was transferred into a quartz UV cell (1 mm) which had been previously evacuated inside a Schlenk tube. A Teflon stopper and Parafilm were then placed on it, avoiding nitrogen bubbles inside the cuvette. All these operations were performed inside the Schlenk tube with a gentle nitrogen flow. The cuvette was then introduced in the thermostated cell compartment of the spectrophotometer, and the kinetic runs were started exactly 3 min after the addition of the catalyst precursor.

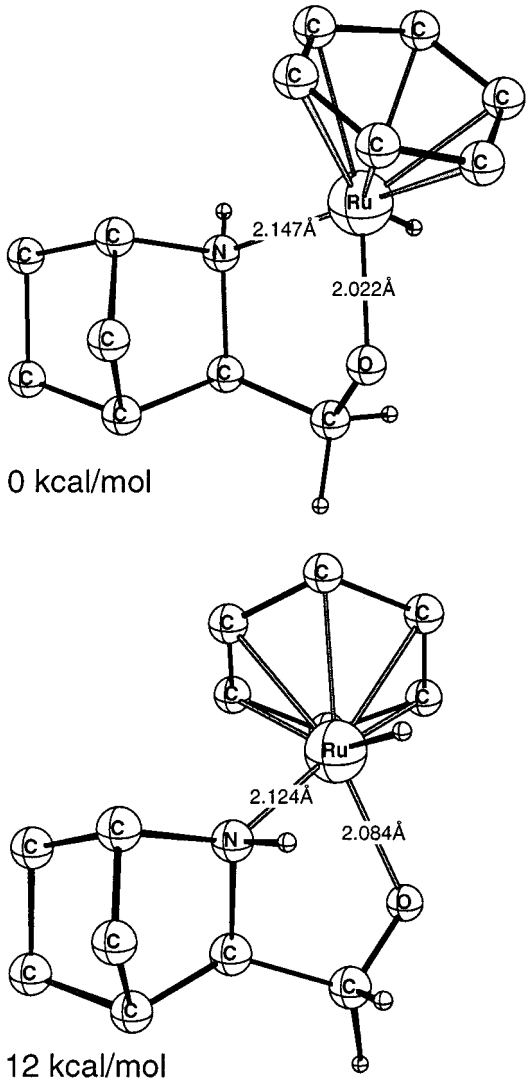

Figure 12. Diastereomeric ruthenium hydrides using ligand **9**. The energy difference is 12 kcal/mol in favor of the diastereomer where the proton at nitrogen is in a *trans* relationship to the carbinol carbon (B3PW91/BS I).

Acknowledgment. We thank the Swedish Natural Science Research Council, the Foundation for Strategic Research (SSF), the Swedish Foundation for International Cooperation in Research and Higher Education (STINT) (postdoctoral fellowship for P.B.), Novartis, and the Swedish Research Council for Engineering Sciences (TFR) for financial support. Access to supercomputer time was provided by the Swedish Council for High Performance Computing (HPDR) and Parallelldatorcentrum (PDC), Royal Institute of Technology.

Supporting Information Available: Structures of intermediates included in Schemes 1 and 2. This material is available free of charge via the Internet at http://pubs.acs.org.

JA9906610